Oil Shale, 2022, Vol. 39, No. 4, pp. 270–289
doi: https://doi.org/10.3176/oil.2022.4.03

Effect of real-time temperature and shear angle on the mechanical strength and energy evolution of oil shale

Siqi Ren[a], Lei Wang[a,b]*, Dong Yang[a,b], Zhiqin Kang[a,b], Pengyu Zhang[a,c]

[a] Key Laboratory of In-situ Property Improving Mining of Ministry of Education, Taiyuan University of Technology, Taiyuan 030024, P. R. China
[b] The In-situ Steam Injection Branch of State Center for Research and Development of Oil Shale Exploitation, Taiyuan University of Technology, Taiyuan 030024, P. R. China
[c] School of Safety and Emergency Management Engineering, Taiyuan University of Technology, Jinzhong, 030600, P. R. China

Received 30 June 2022, accepted 14 October 2022, available online 10 December 2022

Abstract. *During in situ thermal injection in oil shale mining, the shear properties of oil shale at real-time high temperatures considerably affect the stability of injection and production wellbore as well as oil and gas production. The results of this study show that the shear strength and modulus of oil shale decrease with an increase in the shear angle at real-time high temperatures. With increasing temperature, the shear strength and modulus first decrease and then increase, reaching their lowest values at 400 °C. Thereafter, at temperatures above 400 °C, the energy accumulated in the elasticity and crack propagation stages is released and a large amount of energy is liberated during the instability failure. Finally, with rising temperature, the failure stage of oil shale changes from brittle to ductile, secondary fractures gradually increase and the failure characteristics step-by-step turn from through to nonthrough cracking characteristics.*

Keywords: *Balikun oil shale, real-time high temperature, shear angle, shear strength, failure.*

1. Introduction

Oil shale is a sedimentary rock rich in organic matter (kerogen). At high temperatures, solid organic matter is pyrolyzed to generate shale oil and pyrolysis gas [1, 2]. Therefore, oil shale can be used as a supplementary resource for oil. Shale resources are abundant globally, and their efficient

* Corresponding author: e-mail *leiwang0327@163.com*

exploitation is of great significance. Shale oil can be produced via surface retorting and in situ retorting. In the surface retorting technique, oil shale is mined in open-cast quarries or underground mines, and pyrolysis is conducted in retorting furnaces under oxygen-free conditions. However, shale oil yields from surface retorting are extremely low. Moreover, if the orebody is buried deep, the cost of extracting the underground ore and then performing dry distillation on the ground is relatively high [3, 4]. Alternatively, shale oil can be produced in situ through thermal injection.

Oil shale mining by in situ thermal injection is a complex multifold-coupled process of solid-fluid heat-mass transfer. A change in shear strength is an important factor that affects the effectiveness and stability of cementing structures in heat injection and production wells. The shear properties of sedimentary rocks have been widely investigated. Avşar [5] studied the shear parameters and deformation behavior of bimrocks through laboratory-scale direct shear tests, providing a theoretical basis for field testing. Serrano et al. [6] reported a theoretical study on the shear strength of rock joints and derived the relationship between the tangential and normal stresses on joints when the joint surfaces slip. Liang et al. [7] reported that the shear strength, cohesion and internal friction angle of salt rock increase with temperature. These studies on the shear properties of rocks are vital in high-temperature rock mass engineering; however, the shear properties of rock after an elevated temperature is applied do not describe the shear properties under real-time high-temperature conditions.

The mechanical properties of pyrolyzed oil shale have been extensively studied. Zhao and Kang [8] investigated the uniaxial compressive strength of oil shale after being subjected to high temperatures. Zhao et al. [9] conducted triaxial compression tests on oil shale after being subjected to high temperatures. Moreover, few real-time high-temperature tests on the mechanical properties of oil shale have been reported. Yang et al. [10] conducted uniaxial compression tests on oil shale at real-time high temperatures and found that its compressive strength and elastic modulus first decrease and then increase as temperature increases. Yang et al. [11] reported that the tensile strength of oil shale first decreases and then increases with temperature rising. However, real-time analyses of the shear properties of oil shale at high temperatures have not been reported. In the practical application of rock mass engineering, shear failure is an important form of rock mass failure, and compression shear failure is an important factor affecting the safety of rock mass engineering.

In this study, a real-time high-temperature shear experimental system was developed for oil shale variable-angle shear experiments at real-time temperatures. An acoustic emission (AE) system was used to collect the AE characteristic parameters of oil shale during high-temperature shear processes. The variation of shear strength and AE energy with temperature and shear angle during the oil shale shear processes was studied to provide theoretical support for the implementation of oil shale mining via in situ thermal injection.

2. Material and methods

2.1. Sample preparation

The oil shale sample was collected from the Taimu Mining Group in Balikun, Xinjiang. The oil shale was processed into 25 × 25 × 25 mm^3 test pieces. The Balikun oil shale is a low-mature, high-organic source rock, its organic matter is mainly sapropelic; the organic carbon content is 15.64%. Table presents the industrial analysis and Fischer assay retort results of oil shale. Each end face of the test pieces was polished according to the international rock mechanics standards (the end faces of the sample should be strictly parallel, the unevenness should be less than 0.07 mm, and the four side protrusions should be less than 0.03 mm). The temperatures for the experiment were 25 °C, 100 °C, 200 °C, 300 °C, 400 °C, 500 °C and 600 °C, and the shear angles were 45°, 55° and 65°. Three specimens were tested at each temperature and shear angle.

Table. Proximate and Fischer assay analyses of oil shale

Analysis	Composition
Proximate analysis, wt%, ad	
Moisture	1.36
Ash	74.82
Volatile matter	18.48
Fixed carbon	6.70
Fischer assay analysis, wt%, ad	
Oil yield	9.25
Water yield	3.12
Residue	85.58
Gas + loss	2.05

2.2. Test equipment

Figure 1 shows the real-time high-temperature variable-angle shearing system. It is composed of six main components: ① data acquisition system; ② nitrogen atmosphere system; ③ variable-frequency temperature control system; ④ YAW-5T microcomputer-controlled rock pressure testing machine; ⑤ 7-KW electric heating furnace; ⑥ cooling circulation device. The system is used to study the shear properties of oil shale at real-time high temperatures.

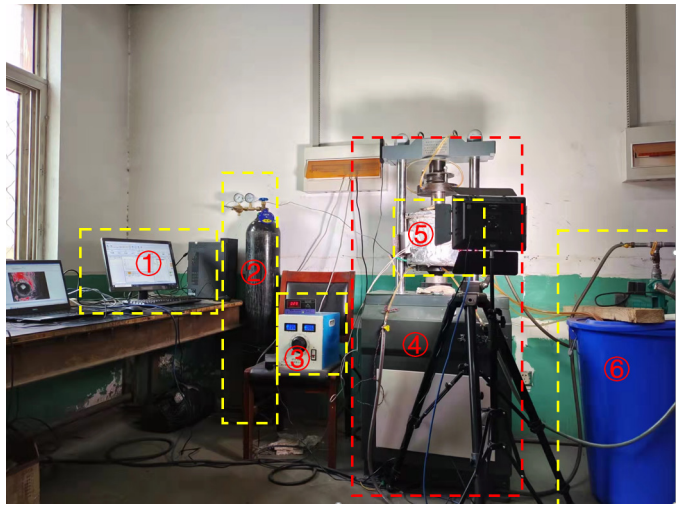

Fig. 1. Real-time high-temperature variable-angle shear test system.

The expansion of pores and fractures and the instability and failure of oil shale during the shear process are accompanied by the absorption, accumulation and release of energy. Monitoring the acoustic emission-ringing number or AE energy (AE signal) during the shear process of oil shale can help us better understand the damage evolution law and crack propagation in oil shale at high temperatures. Figure 2a shows a schematic of the AE detection process. Figure 2b demonstrates PCI-2, a model of the AE device, which is composed of an AE signal-receiving probe, an AE monitor and a display device.

(a)

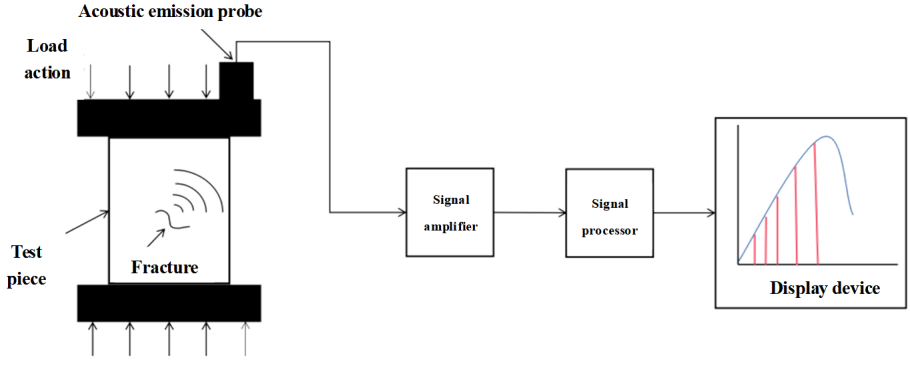

(b)

Fig. 2. (a) Schematic of the acoustic emission detection process; (b) the PCI-2 device.

2.3. Test procedures

The real-time high-temperature shear and AE monitoring experiments carried out with oil shale included the following steps.

1) The heating furnace was placed on the testing machine and the variable-angle shear fixture was placed in it, ensuring that the fixture was at the center of the testing machine. The fixture was adjusted to a 45° shear angle, the test piece was placed in the heating furnace, and a 0.05 kN prestress was applied using the loading system to ensure the overall stability of the fixture.

2) The cooling circulation device was started. The experiment was conducted under nitrogen flow in the electric heating furnace at a flow rate of 0.05 L/min.

3) The temperature control device was switched on and the test piece was heated to the predefined temperature at a heating rate of 1 °C/min. The temperature was maintained for more than 2 h to ensure complete pyrolysis of the test sample.

4) After the AE probe was tightly adhered to the bottom of the loading pedestal of the testing machine, the test piece was subjected to a constant displacement loading of 0.05 mm/min until the specimen was damaged. The test was repeated at shear fixtures with 55° and 65° shear angles.

3. Results and discussion

3.1. Shear stress–strain characteristics of oil shale at real-time high temperatures

In the real-time high-temperature tests, the angle between the shear fixture and the horizontal direction was varied. Considering the friction between the pressure-bearing plate and the fixture, the shear stress of the specimen at shear failure is expressed as follows:

$$\tau = \frac{p}{A_2}\left(\sin\alpha - f\cos\alpha\right),$$

where P is the failure load of the specimen, N; A is the area of the shear surface of the test piece, mm^2; α *is* the shear angle of the test piece, °; and f is the roller friction coefficient.

Figure 3 shows the stress–strain curves of oil shale at different temperatures (from room temperature to 600 °C) and shear angles. The shear stress–strain curves of oil shale samples were basically similar and can be divided into four stages: compaction, elasticity, plasticity and shear failure. The peak shear strain of oil shale at three shear angles gradually increases with increasing temperature. Figures 3a and 3b demonstrate that the shear stress–strain curves of oil shale samples at shear angles of 45° and 55° show a wide linear elasticity stage below 300 °C and the shear failure is brittle. When the temperature exceeds 300 °C, oil shale begins to soften, the compaction stage of the shear stress–strain curve becomes obvious and the plasticity deformation stage gradually increases. The failure of oil shale then changes to the ductile failure and local failure characteristics appear in the plasticity stage. Oil shale at a shear angle of 65° shows the ductile failure at 100 °C and the plasticity deformation stage gradually becomes obvious with increasing temperature (Fig. 3c).

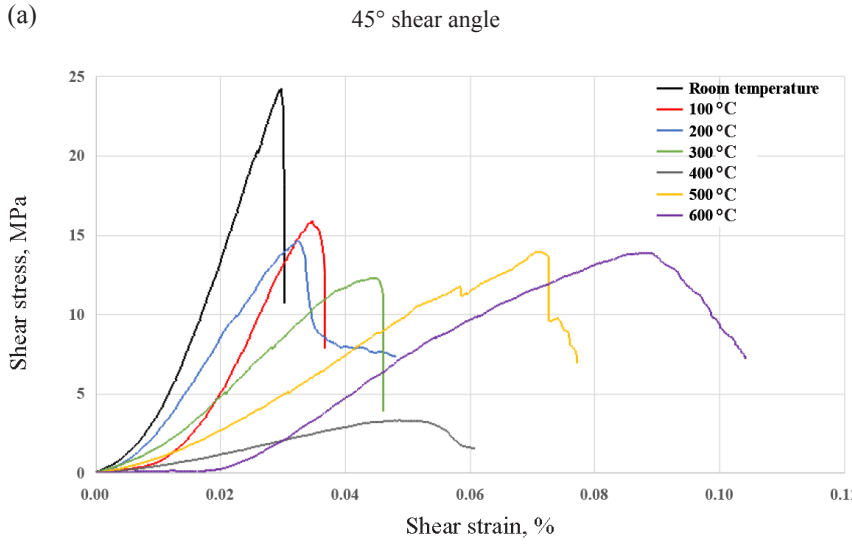

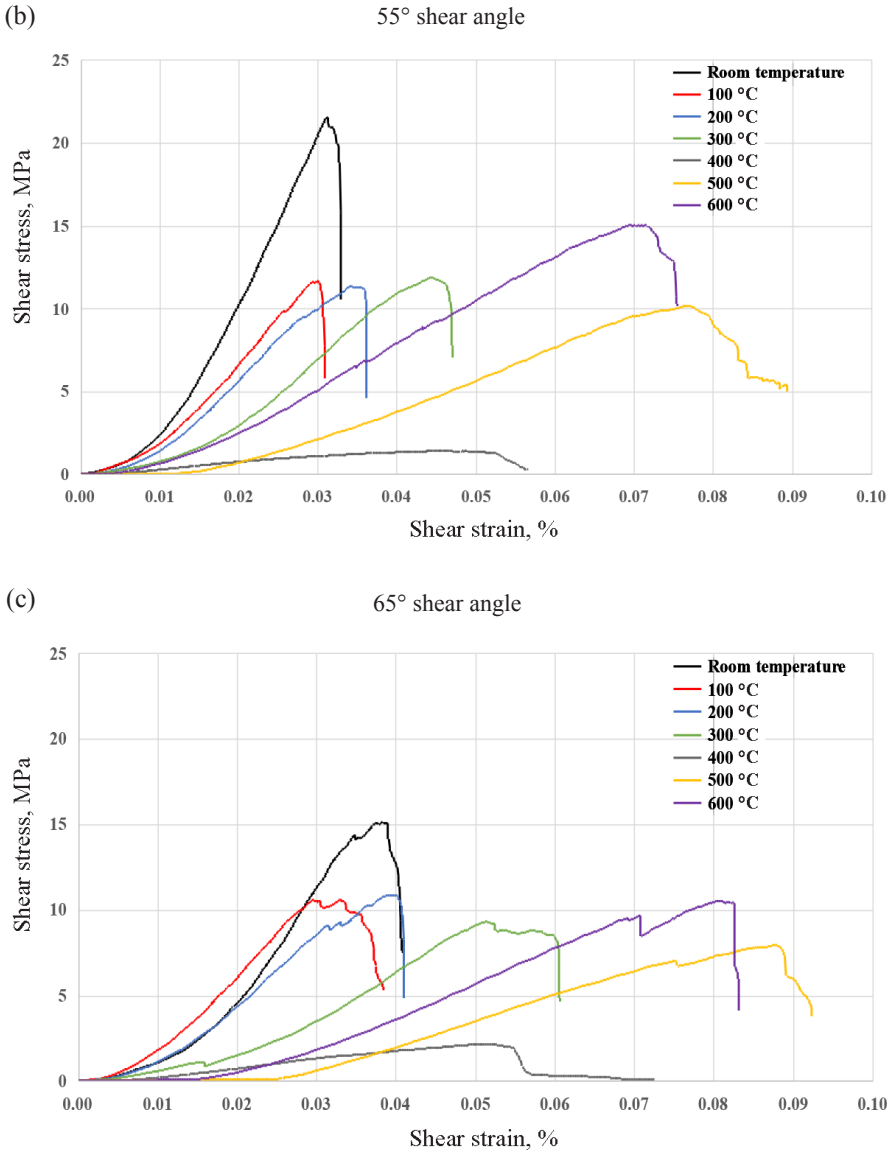

Fig. 3. Variation of shear stress–strain curves of oil shale with temperature.

Figure 4 shows the variation of the shear strength of the oil shale sample with temperature at real-time high temperatures and shear angles of 45°, 55° and 65°. The shear strength of oil shale decreases with increasing shear angle. With an increase in temperature, the shear strength of oil shale decreases first and then increases. The shear strength of oil shale decreases obviously as the temperature increases from room temperature to 200 °C, and the shear

stress decreases by 45%. This is mainly attributed to the expansion pressure generated by water volatilization in this temperature range, which reduces the bond strength between the particles of clay minerals [12, 13], thereby reducing the shear strength. As the temperature rises from 200 °C to 300 °C, the shear strength remains unchanged. On one hand, with an increase in temperature, the internal matrix of oil shale expands due to heating, squeezing the pores and fractures together and thereby improving the strength of oil shale. On the other hand, at 300 °C, the strong binding between the mineral particles in oil shale begins to weaken, making the internal pores and fractures expand along the bedding, thereby reducing the oil shale strength. Therefore, combining these phenomena, the shear strength of oil shale at 300 °C does not change significantly compared with that at 200 °C. With the temperature further increased to 400 °C, the shear strength of oil shale decreases to the lowest value due to the pyrolysis of organic matter. When the temperature reaches 500 °C, the organic matter is pyrolyzed and the lattice of minerals, such as quartz, is transformed, thereby increasing the shear strength of oil shale.

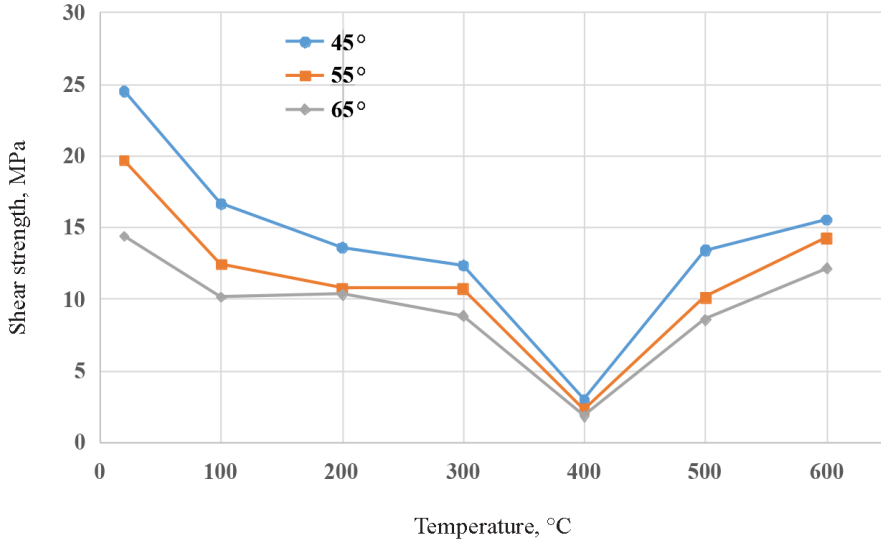

Fig. 4. Variation in the shear strength of oil shale with temperature.

Shear modulus is the ratio of shear stress to shear strain within the limit of elasticity deformation under the action of shear stress. It represents the ability of a material to resist shear strain [14]. Figure 5 shows the variation in the shear modulus of oil shale with temperature. In general, with increasing temperature, the changes in the shear modulus and strength are consistent.

The change in shear modulus with temperature can be divided into two stages.

Stage I, room temperature to 400 °C: in this temperature range, the shear modulus of oil shale decreases rapidly with increasing temperature. When the shear angle is 45°, the shear modulus at room temperature is 45.85 GPa/m, which decreases by 93% as the temperature rises to 400 °C. The decrease in shear modulus is attributed to the same reasons as that in shear strength.

Stage II, 400–600 °C: the shear modulus of oil shale rises slowly with increasing temperature. The shear modulus of oil shale at 500 °C and 600 °C is 10.07 GPa/m and 10.98 GPa/m, respectively, which is approximately 22% and 24% more than that at room temperature. The crystal water existing in the mineral lattice structure in the form of H+ and OH− will dissociate in the high-temperature environment of 400–600 °C, which will lead to the transformation of the mineral lattice and to the increase of the matrix strength. For example, kaolinite is converted into metakaolinite by removing OH−.

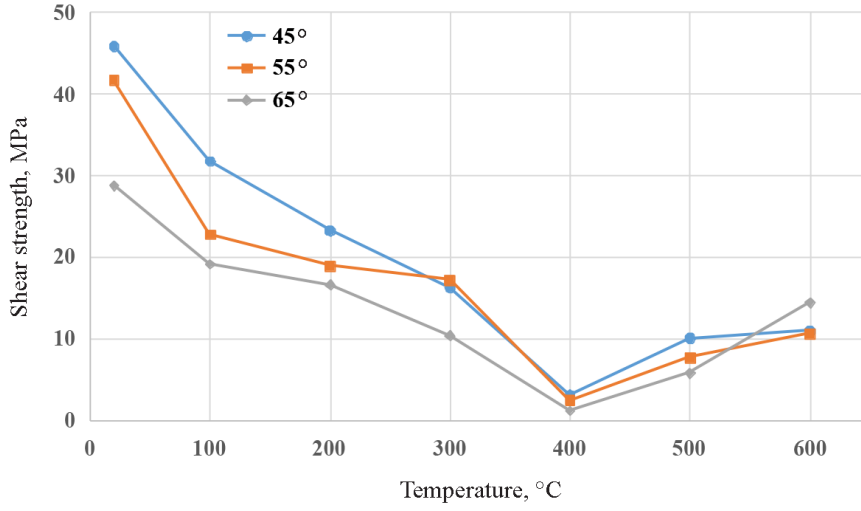

Fig. 5. Variation in the shear modulus of oil shale with temperature.

3.2. Acoustic emission energy of oil shale under shear load at real-time high temperatures

Figure 6 shows the AE energy distribution of oil shale under shear load at different temperatures. The change in AE energy can be divided into four stages: compaction, elasticity, stable crack growth, unstable crack growth. At room temperature, the AE energy of oil shale shows a negligible energy release in the compaction, elasticity and crack propagation stages, indicating no obvious damage to oil shale (Fig. 6a). A large amount of AE energy is released only when the shear failure occurs, and in oil shale there occurs the brittle shear failure.

When the temperature is 100 °C, the AE energy is more active in the entire shear process, as shown in Figure 6b. Compared with the crack propagation stage, the compaction and elasticity stages show an increase in AE energy, indicating the release of the energy accumulated in the pores and fractures in oil shale in the compaction stage, while the shear slip of minerals in the elasticity stage also releases energy. When the temperature is 200 °C, the energy fluctuates for a certain time during the shear process, indicating the presence of relatively few internal pores and fractures (Fig. 6c). The AE energy release at 300 °C (Fig. 6d) is higher than that at 200 °C, while this release is intensive in the entire shear process. When the temperature is 400 °C, the energy accumulated in the elasticity and crack propagation stages is released, while a large amount of energy is liberated at the peak failure (Fig. 6e).

With an increase in temperature, the energy accumulated in the shear process of oil shale increases. Figures 6f and 6g show that when the shear failure occurs in oil shale, the gradually released AE energy increases with an increase in temperature. When the temperature is 500 °C (Fig. 6f), the energy is released throughout the shear process of oil shale, while the energy distribution is relatively small in the stable crack propagation stage. Oil shale softens at 600 °C (Fig. 6g), and as the shear deformation increases, oil shale is compacted and the strength increases. Due to the hardening phenomenon of bedding compaction, large amounts of energy are released during the rock destruction.

(a)

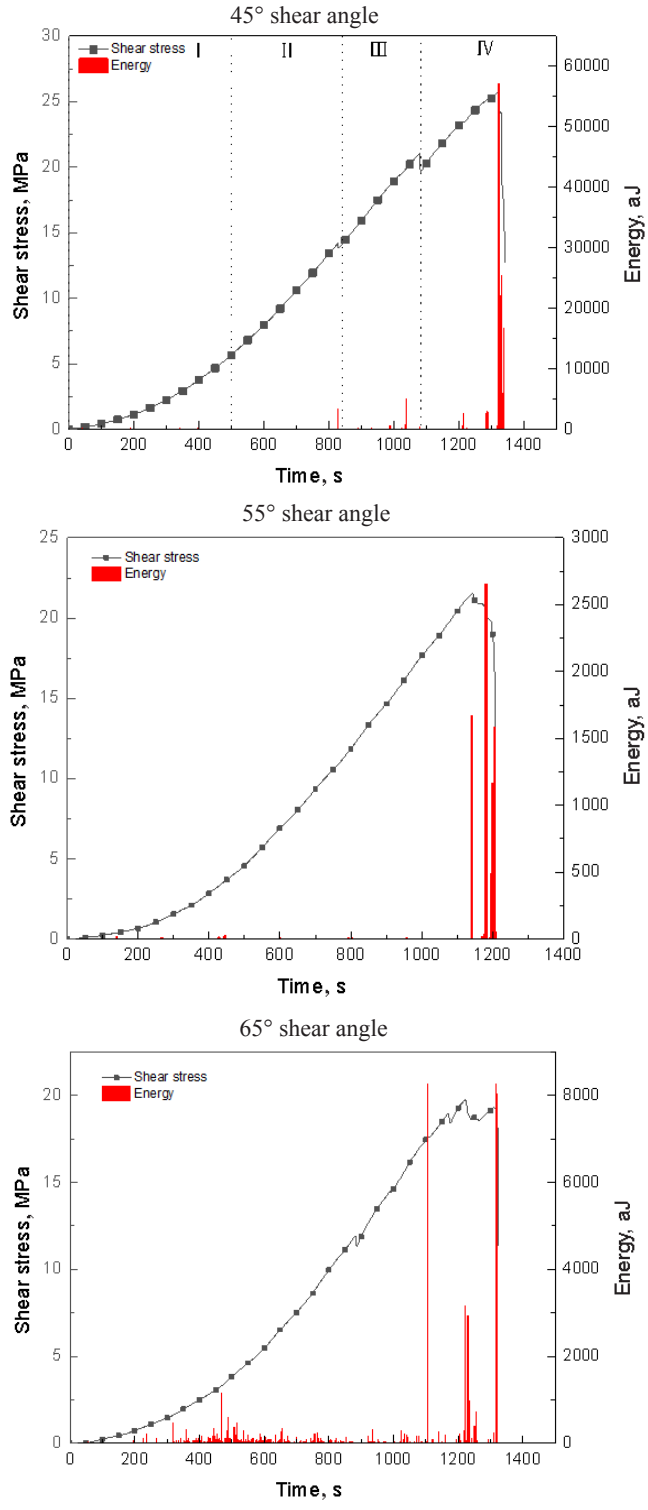
45° shear angle
Shear stress
Energy
Ⅰ
Ⅱ
Ⅲ
Ⅳ
Shear stress, MPa
Energy, aJ
Time, s
55° shear angle
Shear stress
Energy
Shear stress, MPa
Energy, aJ
Time, s
65° shear angle
Shear stress
Energy
Shear stress, MPa
Energy, aJ
Time, s

(b)

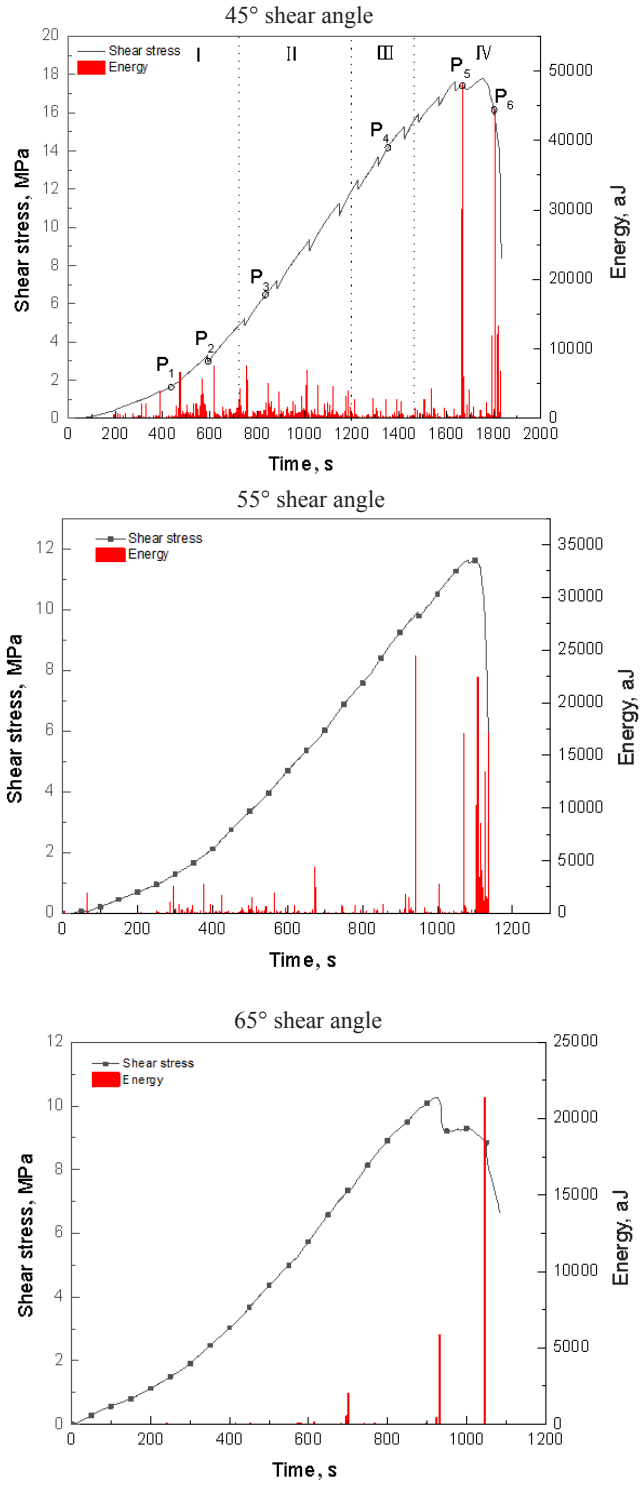
45° shear angle
Shear stress
Energy
I
II
III
IV
P1
P2
P3
P4
P5
P6
Shear stress, MPa
Energy, aJ
Time, s
55° shear angle
Shear stress
Energy
Shear stress, MPa
Energy, aJ
Time, s
65° shear angle
Shear stress
Energy
Shear stress, MPa
Energy, aJ
Time, s

(c)

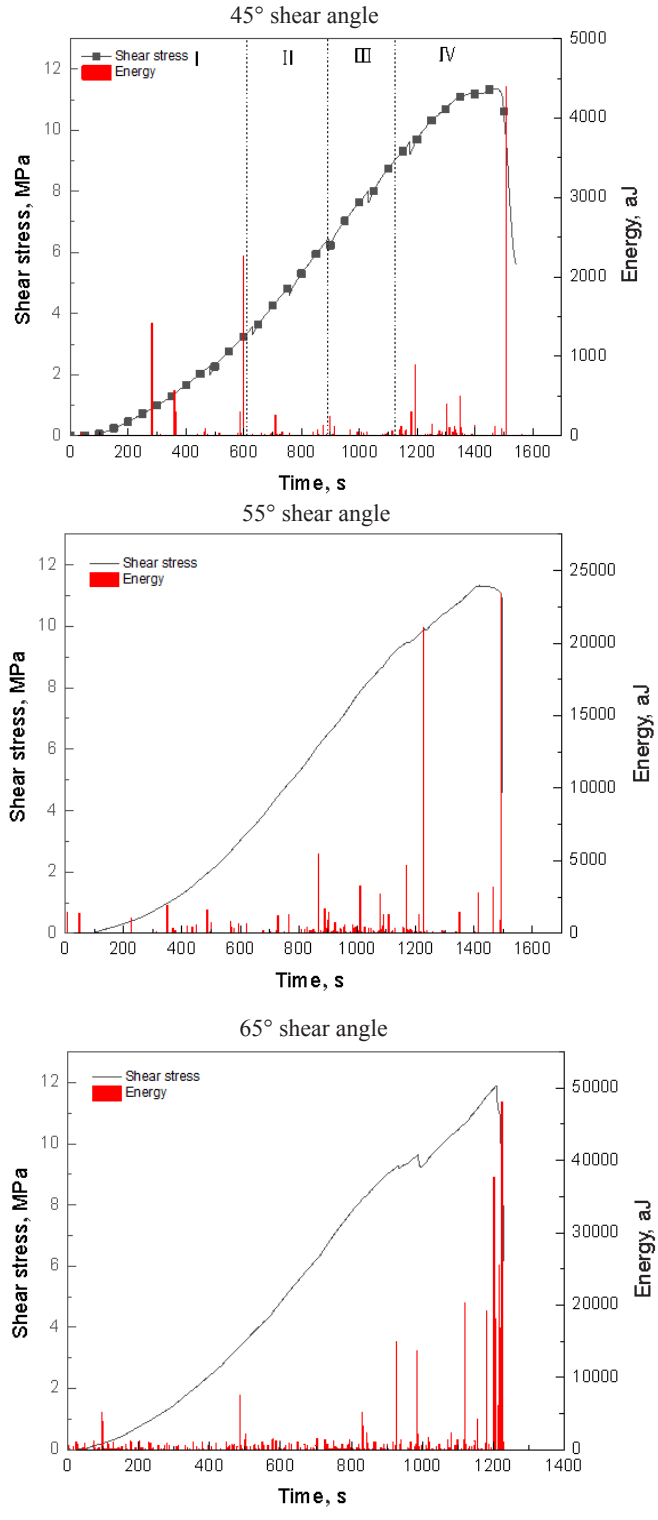
45° shear angle
Shear stress
Energy
I
II
III
IV
Shear stress, MPa
Energy, aJ
Time, s
55° shear angle
Shear stress
Energy
Shear stress, MPa
Energy, aJ
Time, s
65° shear angle
Shear stress
Energy
Shear stress, MPa
Energy, aJ
Time, s

(d)

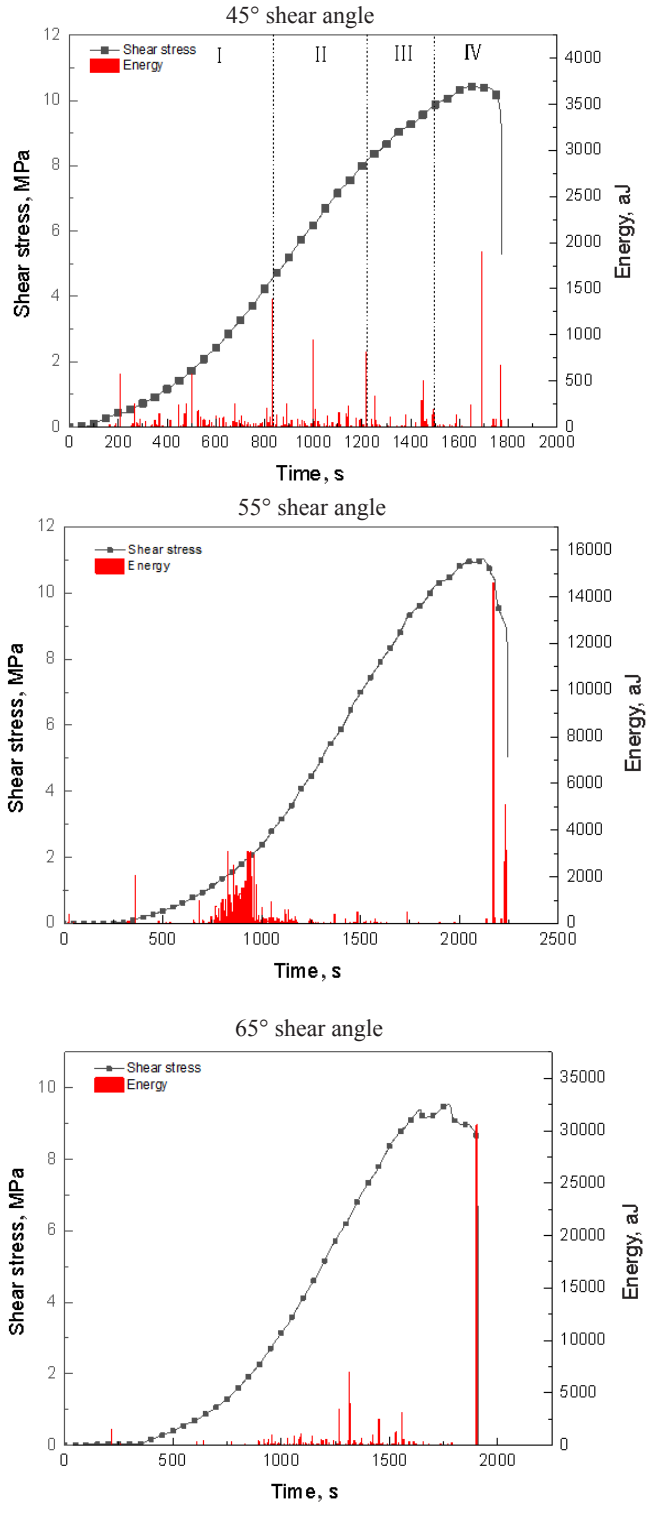
45° shear angle
Shear stress
Energy
I
II
III
IV
Shear stress, MPa
Energy, aJ
Time, s
55° shear angle
Shear stress
Energy
Shear stress, MPa
Energy, aJ
Time, s
65° shear angle
Shear stress
Energy
Shear stress, MPa
Energy, aJ
Time, s

(e)

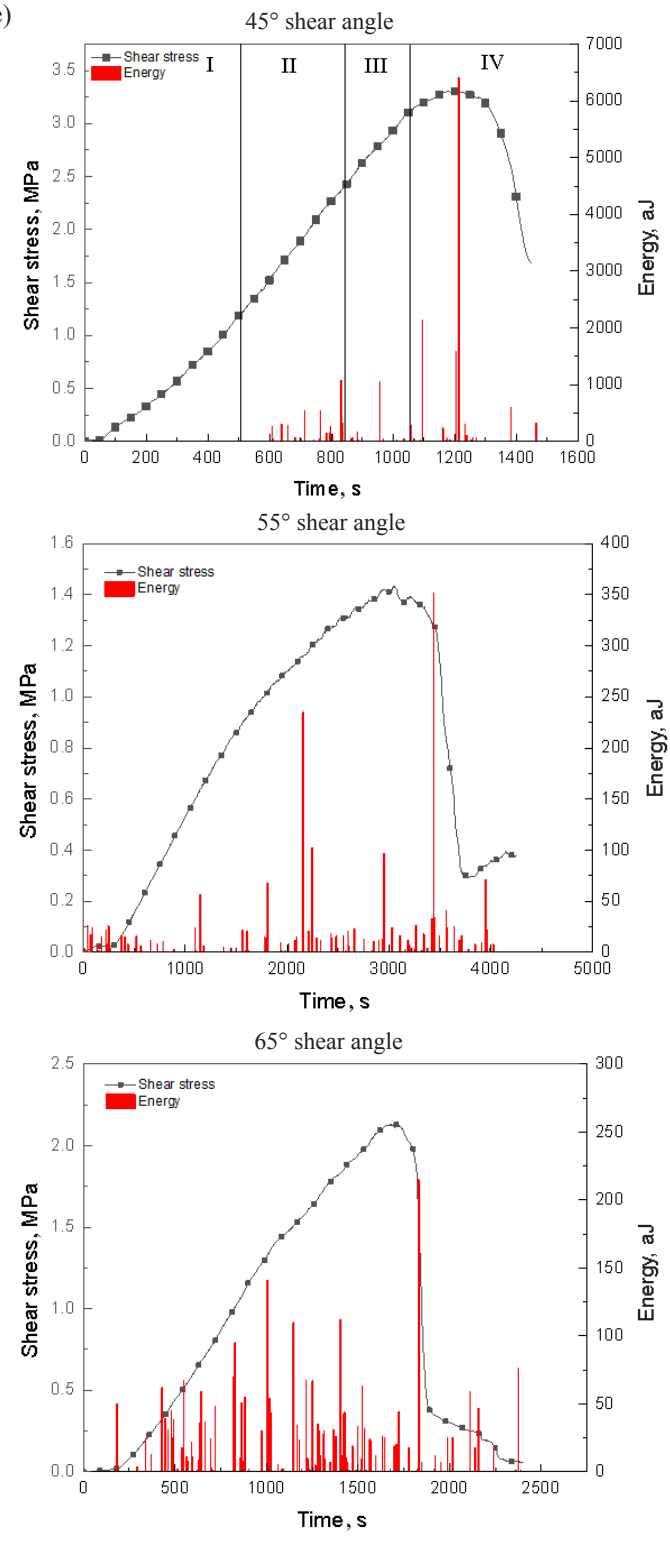
45° shear angle
Shear stress
Energy
I
II
III
IV
Shear stress, MPa
Energy, aJ
Time, s
55° shear angle
Shear stress
Energy
Shear stress, MPa
Energy, aJ
Time, s
65° shear angle
Shear stress
Energy
Shear stress, MPa
Energy, aJ
Time, s

(f)

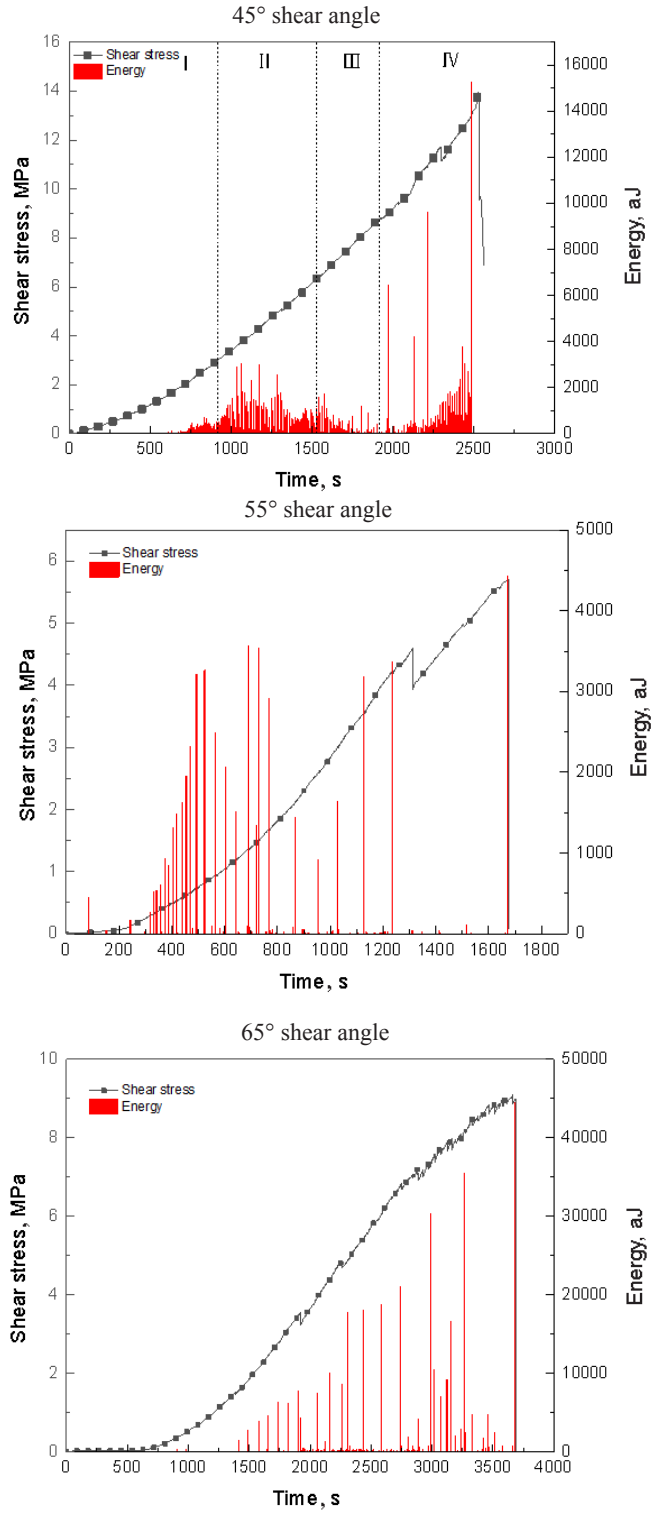
45° shear angle
Shear stress
Energy
I
II
III
IV
Shear stress, MPa
Energy, aJ
Time, s
55° shear angle
Shear stress
Energy
Shear stress, MPa
Energy, aJ
Time, s
65° shear angle
Shear stress
Energy
Shear stress, MPa
Energy, aJ
Time, s

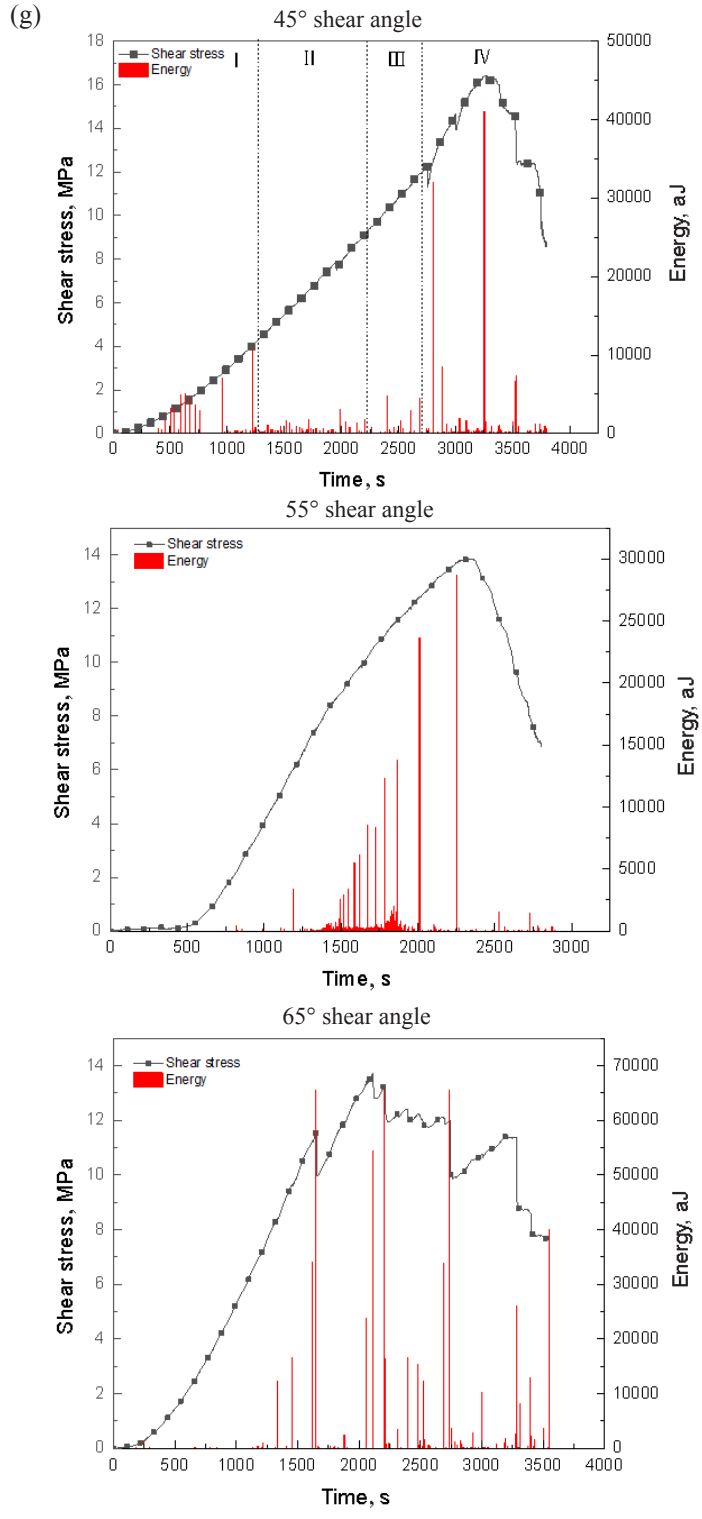

Fig. 6. AE energy in variable-angle shear tests on oil shale at different temperatures: (a) room temperature; (b) 100 °C; (c) 200 °C; (d) 300 °C; (e) 400 °C; (f) 500 °C; (g) 600 °C.

3.3. Shear failure characteristics of oil shale at real-time high temperatures

According to the current classification of rock failure forms, the shear failure forms of oil shale are divided into through, combined and nonthrough crackings [15]. Figure 7 shows the shear failure characteristics of oil shale at a shear angle of 45° at real-time high temperatures. Due to the obvious bedding structure of oil shale, its shear failure at real-time high temperatures is transformed from through to nonthrough cracking. At 100–400 °C, oil shale has an obvious penetrating failure surface (Figs. 7a–d). As the temperature further increases to 500 °C (Fig. 7e), the through cracking characteristics become negligible and the failure characteristics change to the characteristics of nonthrough cracking, which is referred to as combined cracking. At 600 °C (Fig. 7f), oil shale reveals obvious nonpenetrating compression shear failure characteristics. The shear failure starts from the central position, and subsequently, the nonthrough failure occurs along the bedding structure. It can be seen from Figure 7f that numerous secondary cracks are generated in oil shale during the failure process and the number of secondary cracks gradually increases with temperature. The bedding structure of oil shale causes the generation and expansion of secondary fractures with an increase in normal stress. Furthermore, with increasing temperature, a large amount of organic matter is pyrolyzed and the pore structure is formed. The uneven distribution of pores increases the number of secondary fractures in oil shale during the shear process. At 500 °C and 600 °C, oil shale undergoes a remarkable lateral deformation, which is also an important contributor to its nonthrough cracking at high temperatures.

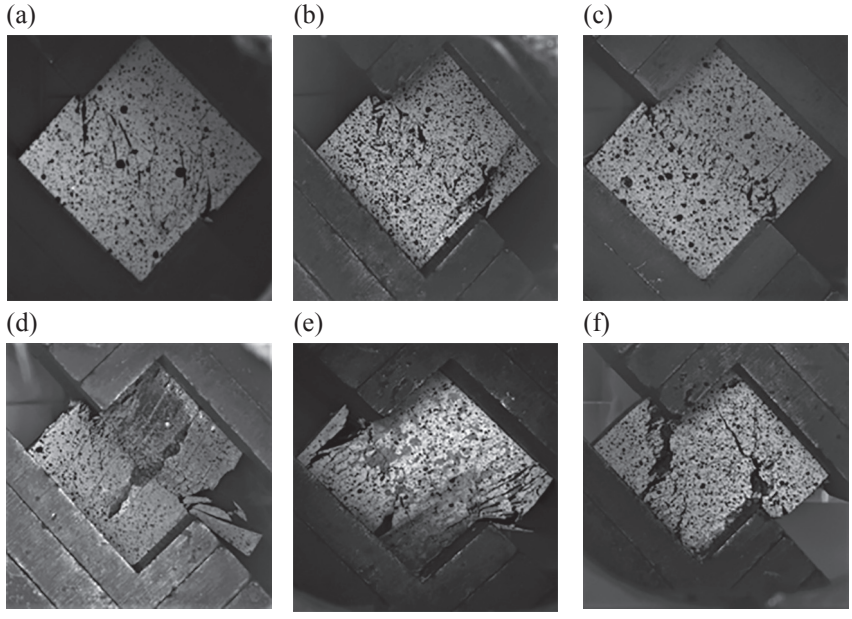

Fig. 7. Shear failure characteristics of oil shale at real-time high temperatures: (a) 100 °C; (b) 200 °C; (c) 300 °C; (d) 400 °C; (e) 500 °C; (f) 600 °C.

4. Conclusions

In this study, a self-designed real-time high-temperature variable-angle shear experimental system and an acoustic emission device were used to study the effects of temperatures and shear angles on the shear mechanical properties and energy evolution of oil shale. The shear failure characteristics of oil shale at different temperatures were analyzed. The following conclusions can be drawn.

1. The stress–strain curves of oil shale at shear angles of 45° and 55° indicate wide linear elasticity stages below 300 °C. When the temperature exceeds 300 °C, the compaction stage gradually becomes obvious, the plasticity deformation increases gradually and the failure of oil shale begins to transform from brittle to ductile. At a shear angle of 65°, oil shale displays the characteristics of ductile failure at 100 °C and the plasticity deformation stage becomes obvious with increasing temperature.

2. The shear strength and modulus of oil shale first decrease and then increase with increasing temperature, reaching their lowest values at 400 °C.

3. The change in the acoustic emission energy during the shear process of oil shale at real-time high temperatures can be divided into four stages: compaction, elasticity, stable crack growth, unstable crack growth. At 100 °C, the AE characteristics of oil shale are relatively dense in the compaction stage due to the precipitation of adsorbed water in it. At 500 °C and 600 °C, due to the sufficient pyrolysis of organic matter, AE in the compaction stage is active.

4. The shear failure characteristics of oil shale change from through to nonthrough cracking characteristics with increasing temperature. The secondary fractures formed in the rock mass during the shear failure process gradually increase with temperature.

Acknowledgments

This study was supported by the National Natural Science Foundation of China (52104144), National Key R&D Program of China (2019YFA0705501), and Basic Research Program of Shanxi Province (20210302124136). We thank Shiyanjia Lab (www.shiyanjia.com) for its linguistic assistance during the preparation of this manuscript.

The publication costs of this article were partially covered by the Estonian Academy of Sciences.

REFERENCES

1. Razvigorova, M., Budinova, T., Petrova, B., Tsyntsarski, B., Ekinci, E., Ferhat, M. F. Steam pyrolysis of Bulgarian oil shale kerogen. *Oil Shale*, 2008, **25**(1), 27–36.

2. Wang, L., Zhao, Y. S., Yang, D., Kang, Z., Zhao, J. Effect of pyrolysis on oil shale using superheated steam: A case study on the Fushun oil shale, China. *Fuel*, 2019, **253**, 1490–1498.
3. Wang, L., Yang, D., Kang, Z. Q., Zhao, J., Meng, Q. R. Experimental study on the effects of steam temperature on the pore-fracture evolution of oil shale exposed to the convection heating. *J. Anal. Appl. Pyrol.*, 2022, **164**, 105533.
4. Al-Ayed, O. S., Hajarat, R. A. Shale oil: Its present role in the world energy mix. *Glob. J. Energ. Technol. Res. Updat.*, 2018, **5**, 11–18.
5. Avşar, E. An experimental investigation of shear strength behavior of a welded bimrock by meso-scale direct shear tests. *Eng. Geol.*, 2021, **294**, 106321.
6. Serrano, A., Olalla, C., Galindo, R. A. Micromechanical basis for shear strength of rock discontinuities. *Int. J. Rock Mech. Min. Sci.*, 2014, **70**, 33–46.
7. Liang, W. G., Xu, S. G., Zhao, Y. S. Experimental study of temperature effects on physical and mechanical characteristics of salt rock. *Rock Mech. Rock Eng.*, 2006, **39**(5), 469–482.
8. Zhao, J., Kang, Z. Q. Permeability of oil shale under in situ conditions: Fushun oil shale (China) experimental case study. *Nat. Resour. Res.*, 2021, **30**(1), 753–763.
9. Zhao, G. J., Chen, C., Yan, H., Hao, Y. L. Study on the damage characteristics and damage model of organic rock oil shale under the temperature effect. *Arab. J. Geosci.*, 2021, **14**(8), 1–12.
10. Yang, D., Wang, G. Y., Kang, Z. Q., Zhao, J., Lv, Y. Q. Experimental investigation of anisotropic thermal deformation of oil shale under high temperature and triaxial stress based on mineral and micro-fracture characteristics. *Nat. Resour. Res.*, 2020, **29**(6), 3987–4002.
11. Yang, S. Q., Yang, D., Kang, Z. Q. Experimental investigation of the anisotropic evolution of tensile strength of oil shale under real-time high-temperature conditions. *Nat. Resour. Res.*, 2021, **30**(3), 2513–2528.
12. Li, M., Wang, D., Shao, Z. Experimental study on changes of pore structure and mechanical properties of sandstone after high-temperature treatment using nuclear magnetic resonance. *Eng. Geol.*, 2020, **275**, 105739.
13. Tang, Z. C., Zhang, Q. Z., Peng, J., Jiao, Y. Y. Experimental study on the water-weakening shear behaviors of sandstone joints collected from the middle region of Yunnan province, P.R. China. *Eng. Geol.*, 2019, **258**, 105161.
14. Geng, Z., Chen, M., Jin, Y., Yang, S., Yi, Z., Fang, X., Du, X. Experimental study of brittleness anisotropy of shale in triaxial compression. *J. Nat. Gas Sci. Eng.*, 2016, **36**, Part A, 510–518.
15. Du, K., Li, X., Wang, S., Tao, M., Li, G., Wang, S. Compression-shear failure properties and acoustic emission (AE) characteristics of rocks in variable angle shear and direct shear tests. *Measurement*, 2021, **183**, 109814.